High-Bandwidth Hybrid Quantum Repeater

W. J. Munro,[1,2,*] R. Van Meter,[2,3] Sebastien G. R. Louis,[2,4] and Kae Nemoto[2]

[1]*Hewlett-Packard Laboratories, Filton Road, Stoke Gifford, Bristol BS34 8QZ, United Kingdom*
[2]*National Institute of Informatics, 2-1-2 Hitotsubashi, Chiyoda-ku, Tokyo 101-8430, Japan*
[3]*Keio University, 5322 Endo, Fujisawa, Kanagawa, 252-8520, Japan*
[4]*Department of Informatics, School of Multidisciplinary Sciences, The Graduate University for Advanced Studies,*
2-1-2 Hitotsubashi, Chiyoda-ku, Tokyo 101-8430, Japan

We present a physical- and link-level design for the creation of entangled pairs to be used in quantum repeater applications where one can control the noise level of the initially distributed pairs. The system can tune dynamically, trading initial fidelity for success probability, from high fidelity pairs ($F = 0.98$ or above) to moderate fidelity pairs. The same physical resources that create the long-distance entanglement are used to implement the local gates required for entanglement purification and swapping, creating a homogeneous repeater architecture. Optimizing the noise properties of the initially distributed pairs significantly improves the rate of generating long-distance Bell pairs. Finally, we discuss the performance trade-off between spatial and temporal resources.

Quantum information has reached a very interesting stage in its development, where we have seen many fundamental experiments laying the foundation for practical systems [1]. Now certain applications, such as quantum key distribution (QKD), are being readied for commercial use [2,3], where practical distances hover around the 150 km mark. Any quantum communication longer than this limit suffers severely from noise and exponential loss in the quantum communication channel. Hence, the quantum communication for either QKD over a distance beyond the limit, or more generally, all distributed quantum information processing, requires the development of a high-bandwidth repeater which can distribute and potentially process quantum information given these constraints. In a quantum repeater system, initial imperfect Bell pairs (which we call base-level pairs) are distributed over channel segments. These base pairs are then purified to high fidelity Bell pairs and connected via entanglement swapping, resulting in entanglement between the qubits at distant stations. Iterating this procedure creates Bell pairs at even larger distances. These pairs can be used in many different applications, including QKD, quantum communication, distributed quantum computation, and quantum metrology and related uses [4–8].

The many recently proposed schemes for the design of a quantum repeater fall into two categories. The majority of the schemes focus on the heralded creation of very high fidelity base-level pairs [9–17]. For longer segment lengths, the generation of these high fidelity pairs comes at the expense of a very low probability of success, which becomes one of the major bottlenecks in the overall performance of a repeater system. Another significant issue is that in the majority of these schemes, local gates between multiple qubits within a single repeater station are difficult. An alternative approach has recently been proposed, instead creating base-level pairs of moderate fidelity and

high heralded success probability [18,19]. In this second approach, the physical resources used for long-distance entanglement also efficiently implement local gates, facilitating the purification of moderate fidelity pairs back to high fidelity pairs. For instance, with 16 qubits per node with a 10 km spacing rate, 15 pairs of fidelity $F = 0.98$ can be achieved over a 1280 km repeater network; however, at longer repeater node spacing distances (>40 km) the rate falls to zero. This node spacing issue is one of the key limitations for this second approach. These two approaches are radically different in the use of physical resources and in technological requirements. It is hence not trivial to directly compare the feasibility and efficiency of schemes in different approaches. However, it has been thought that these two approaches are complementary to each other, trading high fidelity for high success probability or vice versa. Quantum repeaters of the latter kind typically use coherent light instead of the single photons common in the former category. It has been believed that a coherent-light quantum repeater is fundamentally unable to generate high fidelity Bell pairs and hence is unable to cope with severe loss in the quantum channel. In this Letter we address this shortcoming by presenting the design of a new scheme for entanglement distribution utilizing coherent light and demonstrate that in fact such a system is more flexible over a wide range of losses without serious overhead in physical resources. This advance will have a significant impact on the overall repeater performance.

In this Letter we consider the design of a repeater segment where one can dynamically vary the quality of the base-level entangled pairs from very high to moderate fidelity. This tunability will allow one to trade the fidelity of the entangled pairs against the probability of their successful distribution for a given segment length. We will also ensure that the same physical resources can be used to implement the local gates necessary for the entan-

glement purification and entanglement swapping [20,21]. In this case, both requirements can be met via a controllable interaction between our qubit and light field.

The core interaction between our qubit and field in our cavity quantum electrodynamics system is the Jaynes-Cummings (JC) Hamiltonian given by $H_{JC} = \hbar g(a^\dagger \sigma_- + a\sigma_+)$ where $2g$ is the vacuum Rabi splitting for the dipole transition. a ($a^\dagger$) refers to the annihilation (creation) operators of the electromagnetic field mode in a cavity and σ_+ (σ_-) the raising (lowering) operators of the qubit with ground state $|0\rangle$ and excited state $|1\rangle$. Our qubit is a solid-state electronic spin which is also coupled to a nuclear spin qubit, allowing for a coherent transfer of quantum information to the long-lived nuclear spin qubit. Physically, the electronic and nuclear spin systems may be achieved, for example, by single electrons trapped in quantum dots, nitrogen vacancy centers in diamond, or neutral donor impurities in semiconductors.

Our basic JC Hamiltonian can be used to implement a controlled displacement $D(\beta\sigma_z) \equiv e^{\sigma_z(\beta a^\dagger - \beta^* a)}$ operation [21,22] between the qubit and field, where $\sigma_z = |0\rangle\langle 0| - |1\rangle\langle 1|$. This operation displaces the field mode by an amount β conditioned on the state of the qubit. There are a number of ways this interaction can be achieved ranging from shaped pulse sequences modulating the qubit or field [23] to sequences of controlled rotations and unconditional displacement operations [22].

These controlled displacement operations now form the basis of an efficient and tunable entanglement distribution scheme, as depicted in Fig. 1. The scheme works as follows: our first qubit is prepared in an equal superposition of both basis states $(|0\rangle + |1\rangle)/\sqrt{2}$ with the probe mode in the cavity initially being the vacuum. The qubit interacts with the probe beam via the controlled displacement operation $D(\beta\sigma_z)$ resulting in the combined qubit-probe state $(|0\rangle|\beta\rangle + |1\rangle|-\beta\rangle)/\sqrt{2}$. The probe beam is either switched out or leaks out of the cavity and is transmitted over the noisy loss channel to the second cavity. Here the second qubit and probe mode interact via a controlled displacement operation. The probe beam then leaks out of this second cavity and is measured, projecting our qubits into an appropriate entangled state. In more detail, if our

Phase Reference

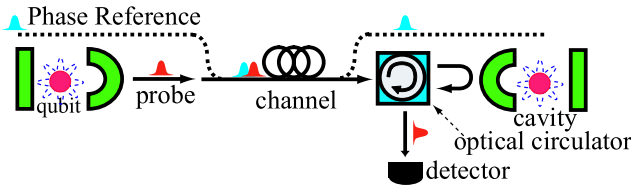qubit · probe · channel · cavity · optical circulator · detector

FIG. 1 (color online).   Schematic of an entanglement distribution scheme based on two qubits in individual cavities interacting indirectly via a shared probe beam and controlled displacement operations. An optical circulator before the second qubit routes the probe field into the cavity and the resulting beam leaking out to the detector. A phase reference is sent along the same lossy channel.

two distributed qubits are prepared in a state $(|00\rangle + |01\rangle + |10\rangle + |11\rangle)/2$, then after both controlled displacements and the noisy channel our two qubit-light field state can be represented by

$$\rho = \frac{1 + e^{-\bar{\gamma}/2}}{2}|Z_+\rangle\langle Z_+| + \frac{1 - e^{-\bar{\gamma}/2}}{2}|Z_-\rangle\langle Z_-|, \quad (1)$$

where $|Z_\pm\rangle = \frac{\sqrt{\mathcal{N}_\pm}}{2}|\Phi_+\rangle|c_\pm\rangle + \frac{\sqrt{\mathcal{N}_\mp}}{2}|\Phi_-\rangle|c_\mp\rangle + \frac{1}{\sqrt{2}}|\Psi_\pm\rangle|0\rangle$, $|\Phi_\pm\rangle = |\frac{00\pm11}{\sqrt{2}}\rangle$, $|\Psi_\pm\rangle = |\frac{01\pm10}{\sqrt{2}}\rangle$, $|c_\pm\rangle = (|2\beta e^{-l/2l_0}\rangle \pm |-2\beta e^{-l/2l_0}\rangle)/\sqrt{2\mathcal{N}_\pm}$ with $\mathcal{N}_\pm = 1 \pm \exp[-8|\beta|^2 e^{-l/l_0}]$ and $\bar{\gamma} = 2|\beta|^2(1 - e^{-l/l_0})$. Here l/l_0 represents the attenuation of the probe in the channel. Now the probe beam in Eq. (1) is in one of three possible states, $|c_\pm\rangle$ or the vacuum $|0\rangle$. The odd cat state $|c_-\rangle$ is orthogonal to both $|c_+\rangle$ and $|0\rangle$. However, $|c_+\rangle$ and $|0\rangle$ are nonorthogonal with an overlap $2\exp[-4|\beta|^2 e^{-l/l_0}]/(1 + \exp[-8|\beta|^2 e^{-l/l_0}])$. Of course, if $\beta e^{-l/2l_0} \gg 1$, these two states are effectively orthogonal, and so one could distinguish all probe beam states. However, the channel loss has had two significant effects. First, it has mixed $|Z_+\rangle$ with $|Z_-\rangle$ with a mixing parameter $\frac{1 + e^{-\bar{\gamma}/2}}{2}$. This mixing parameter is small only when $|\beta|^2(1 - e^{-l/l_0}) \ll 1$, which is in conflict with the desire to have all probe beam states nearly orthogonal for channels of moderate length. Second, the channel has also attenuated the probe beam's amplitude and so the second controlled displacement must be by $D(\beta e^{-l/2l_0}\sigma_{z_2})$ rather than $D(\beta\sigma_{z_2})$ to minimize the effect of the loss.

We now turn our attention to the measurement of the probe and the resulting conditioning it causes on the distributed qubits. There are various measurement strategies, ranging from highly idealized cat state projectors (CSP) $|c_-\rangle\langle c_-|$ to single-photon detection (SPD). Using such detection strategies, our qubits are conditioned to

$$\rho(F) = F|\Phi_-\rangle\langle\Phi_-| + (1 - F)|\Phi_+\rangle\langle\Phi_+| \quad (2)$$

with heralded success probabilities

$$P_{CSP}[F] = \frac{1}{4}\{1 - [2F - 1]^{8e^{-l/l_0}/(1-e^{-l/l_0})}\} \quad (3)$$

$$P_{SPD}[F] = \frac{1}{2}\frac{d}{d\lambda}[2F - 1]^{\{4\eta^2 e^{-l/l_0}/[1+(7-8\eta^2)e^{-l/l_0}]\}\lambda}\bigg|_{\lambda=1}, \quad (4)$$

respectively. The single-photon detector is assumed to have a nonunit quantum efficiency η^2. Equations (2)–(4) have been expressed in terms of the fidelity F of the $|\Phi_-\rangle$ state generated, the attenuation parameters l/l_0, and the detection efficiency rather than β. The initial displacement β can be expressed in terms of F, l/l_0, P, and η^2. We also need to point out that Eq. (2) is a mixture of only two Bell states, $|\Phi_\pm\rangle$, which has important advantages in entanglement purification. Such states are much more efficient to purify.

In Fig. 2 we plot these probabilities $P[F]$ versus fidelity for both measurement strategies (with $\eta^2 = 0.9, 1$) for an

attenuation length $l/l_0 = 0.8$. Our idealized cat projector (CSP) allows a nice range of fidelities to be achieved, ranging from $F = 1/2$ to $F = 1$. For higher fidelities, lower success probabilities are achieved. The major issue with the cat projector is that it is difficult to implement in practice, but for the moderate to high fidelity regimes, the single-photon detection scheme closely follows the cat projector results and so is an excellent compromise. It also highlights that single photons (and hence single-photon sources) are not needed for creating high fidelity distributed Bell pairs. The sending of coherent states (whether weak or strong) can achieve the same goal. High fidelity pairs can be generated over long distances but at the expense of the success probability. Other measurement techniques (such as homodyne, bucket, or vacuum detection) also result in entangled states, but these states tend be composed of more than two Bell states, and so are more difficult to purify. However, they can provide success probabilities greater than one-half but result in low fidelity final states.

We now have a highly tunable segment where one can dynamically vary the quality of the base-level entangled pair from low to high fidelity utilizing nonunit efficiency single-photon detection. These pairs can be used in a repeater protocol to create long-distance entangled pairs. The basic repeater protocol works as follows: multiple copies of lower fidelity base-level pairs are purified to create high fidelity pairs, then entanglement swapping of the high fidelity pairs between adjacent repeater nodes creates longer distance but lower fidelity pairs. These resulting pairs can then be purified to high fidelity pairs and entanglement swapping gives even longer range pairs. The procedure is iterated until pairs over the desired length are obtained. The purification and entanglement swapping protocols require efficient local two-qubit C-Z (or CNOT) gates. In our architecture these can be achieved using another sequence of controlled displacement operations $D(i\beta_2\sigma_{z2}) \times D(\beta_1\sigma_{z1})D(-i\beta_2\sigma_{z2})D(-\beta_1\sigma_{z1}) \equiv \exp[2i\beta_1\beta_2\sigma_{z1} \otimes \sigma_{z2}]$ with β_1 and β_2 satisfying $\beta_1\beta_2 = \pi/8$ [21,22]. These quantum bus (qubus) based local gates are needed
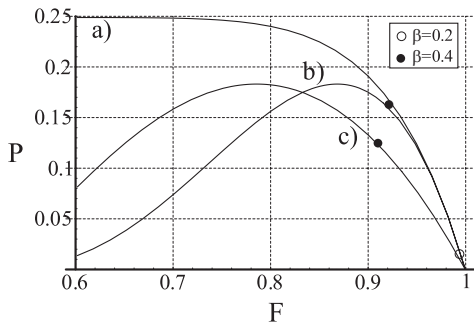

FIG. 2. Plot of the probability $P[F]$ of successfully establishing an entangled pair at an attenuation length of $l/l_0 = 0.8$ (20 km in commercial fiber) versus fidelity for the different measurement strategies: (*a*) odd state cat projector CSP, (*b*) ideal SPD, and (*c*) SPD with $\eta^2 = 0.9$.

throughout the protocol, and so the more efficient and robust they are the better our overall performance.

One of the major issues for performance becomes the chosen quality of base-level entangled pairs for our lowest-level segment. Conventional quantum repeater wisdom generally suggests that before one performs entanglement swapping to create longer pairs, one should purify the noisy base-level pairs as best as possible. For our discussions here we will set a working fidelity of $F = 0.98$ before attempting entanglement swapping. There are now a number of ways we can use our tunable segment to achieve this required fidelity. We could just directly create a pair of that fidelity, or we could create lower fidelity pairs and purify them using standard protocols [24–27]. Which approach is best will depend on both the probability of generating the entangled pairs P_g and the purification probability P_{pur}. For a one-round purification protocol with no limitation on the physical resources, the effective probability of generating the final fidelity pair (per channel) is given by $P_{eff} = P_g P_{pur}/2$. The purification probability depends critically on the form of the initial entangled pairs, and so our engineering of Eq. (2) above is very advantageous. A mixture of two Bell states is much easier to purify than more general mixed states. In this situation, two copies of $\rho(F)$ can be purified to a new entangled $\rho[F' = F^2/(1 - 2F + 2F^2)]$ with a $P_{pur}(F) = F^2 + (1 - F)^2$ [27]. This gives an overall probability of success for generating a $F = 0.98$ pair from two $F = 0.9$ pairs of $P_{eff} = 0.0547$. In comparison, we have generation probabilities of 0.033 74 for directly manufacturing the $F = 0.98$ pair. Thus, using lower fidelity pairs and purification improves our overall probability of generating the final pair, assuming efficient local gates.

Does a multiple-round purification protocol improve our results? Moving to multiple rounds, there are a number of choices for how to implement the protocol [24,26]. As an illustration, consider a symmetric purification protocol [26] where four $F = 0.75$ pairs are purified to the $F = 0.98$ pair. In this case, we have an effective generation probability of $P_g = 0.0236$ which is lower than the probability achieved by the single-round protocol. The difference is primarily due to the lower probability of successfully purifying lower fidelity pairs.

We now need to turn our attention to a more detailed discussion of the physical resources required for creating our long-distance pairs. It is important to consider both the spatial and temporal resources necessary. The tunability of our source allows us significant flexibility in how we use resources. We can implement the minimum physical resource strategies (two qubits per station) developed by Childress *et al.* [11], as well as the modest physical resource 16 qubit per station schemes of van Loock *et al.* [18] and Ladd *et al.* [19]. Because of our low to moderate probabilities of successfully creating the base pairs between stations, the minimum physical resource approach will have significant performance issues due to this distri-

TABLE I. Rate of final generation of distant $51.2l/l_0$ (1280 km) entangled pairs of minimum fidelity $F = 0.98$ resulting from a nested entanglement protocol with 8, 16, and 32 qubits per half-station. The stations are separated by either $0.4l/l_0$, $0.8l/l_0$, or $1.6l/l_0$ attenuation lengths. The number in the brackets indicates the total numbers of qubits over all repeater stations. We have assumed an initial fidelity reduction in the base pairs due to loss in the fiber (assumed to be 0.17 dB/km) and distortion of 0.1% due to local losses during the measurement-free displacement-based C-Z gate.

Qubits half-station	$0.4l/l_0$	$0.8l/l_0$	$1.6l/l_0$
8	520 (2048)	693 (1024)	193 (512)
16	1097 (4096)	1528 (2048)	437 (1024)
32	2297 (8192)	3190 (4096)	987 (2048)

bution bottleneck. Significant time will be spent idle waiting for the base pairs to be successfully created between all stations. However, by allowing moderate physical resources, we can simultaneously attempt to create multiple base pairs per segment, and so reduce the time waiting for the necessary resources to become available. This approach will dramatically increase the throughput of the entire repeater chain. To quantify this degree of the improvement, we have performed a Monte Carlo simulation of a nested entanglement protocol over $51.2l/l_0$ (1280 km) for varying numbers of qubits per station with dynamical resource allocation [28]. The results are presented in Table I. First, they show that, of the three segment lengths considered, the best results were obtained from the $0.8l/l_0$ (20 km) situation. For longer distances, the initial success probability drops dramatically, and for shorter segment lengths, errors in local gates have a significant impact. We also found that the protocol could run with local gate error rates exceeding 1%, though in this situation the generation rate falls to only a few pairs per second. Raising the number of qubits in each half-station also gives a slight improvement compared to stacking smaller repeater nodes in parallel. Still, our results show a good generation rate with 8–16 qubits per half node. In the scheme of van Loock, with 16 qubits per half node with $0.4l/l_0$ segment spacing (4096 total qubits), a rate of 15 $F = 0.98$ Bell pairs per second was achieved. Using our new scheme (for the same total number of qubits), we achieve a rate of 3190 pairs per second, an improvement of over 2 orders of magnitude. Our new scheme also produces relatively high throughput of 437 pairs at a link distance of 40 km compared with zero for the original van Loock case. In the new scheme, the fidelity remains high over long distances, but the probability of success declines. Finally, some of our improvements in the protocol are obtained by tuning the base-level fidelity to optimize the number of purification rounds before entanglement swapping.

In summary, we have shown how to implement a high-bandwidth quantum repeater using the fundamental atom-light interactions in quantum optics, through a qubus-mediated entangling operation. This new approach refutes the criticism that hybrid repeaters cannot adapt to a wide range of losses and offers flexibility on fidelity and entanglement success probability. In this hybrid scheme, the only required interactions are controlled displacement operations between the light field and qubit. These controlled displacement operations result in the distribution of moderate to high fidelity entanglement between the qubits in the repeater stations, conditioned on single-photon detection of the qubus mode. They also can implement a deterministic C-Z gate for use in all the purification and entanglement swapping steps. Such tools allow for the natural design of a scalable and homogeneous quantum repeater network and thus a distributed computation with many concurrent steps happening in different locations. Using high-efficiency single-photon detection, we have shown that long-distance communication rates over 1000 pairs per second with a fidelity above 98% are possible with only modest resources.

*bill.munro@hp.com
[1] T. P. Spiller *et al.*, Contemp. Phys. **46**, 407 (2005).
[2] N. Gisin *et al.*, Rev. Mod. Phys. **74**, 145 (2002).
[3] J. L. Duligall *et al.*, New J. Phys. **8**, 249 (2006).
[4] R. Van Meter *et al.*, ACM J. Emerging Technol. Comput. Syst. **3**, 1 (2008).
[5] J. I. Cirac *et al.*, Phys. Rev. A **59**, 4249 (1999).
[6] L. K. Grover, arXiv:quant-ph/9704012.
[7] A. Serafini *et al.*, Phys. Rev. Lett. **96**, 010503 (2006).
[8] I. L. Chuang, Phys. Rev. Lett. **85**, 2006 (2000).
[9] H.-J. Briegel *et al.*, Phys. Rev. Lett. **81**, 5932 (1998).
[10] W. Dür *et al.*, Phys. Rev. A **59**, 169 (1999).
[11] L. Childress *et al.*, Phys. Rev. Lett. **96**, 070504 (2006).
[12] A. Klein *et al.*, Phys. Rev. A **73**, 012332 (2006).
[13] S. J. Enk *et al.*, Science **279**, 205 (1998).
[14] L.-M. Duan *et al.*, Nature (London) **414**, 413 (2001);
[15] Z.-B. Chen *et al.*, Phys. Rev. A **76**, 022329 (2007).
[16] B. Zhao *et al.*, Phys. Rev. Lett. **98**, 240502 (2007).
[17] L. Jiang *et al.*, Phys. Rev. A **76**, 012301 (2007).
[18] P. van Loock *et al.*, Phys. Rev. Lett. **96**, 240501 (2006).
[19] T. D. Ladd *et al.*, New J. Phys. **8**, 184 (2006).
[20] K. Nemoto and W. J. Munro, Phys. Rev. Lett. **93**, 250502 (2004).
[21] T. P. Spiller *et al.*, New J. Phys. **8**, 30 (2006).
[22] P. van Loock *et al.*, arXiv:quant-ph/0701057.
[23] D. F. Walls and G. J. Milburn, *Quantum Optics* (Springer, New York, 2008), 2nd ed.
[24] W. Dür and H. J. Briegel, Rep. Prog. Phys. **70**, 1381 (2007).
[25] C. H. Bennett *et al.*, Phys. Rev. Lett. **70**, 1895 (1993).
[26] W. Dür *et al.*, Phys. Rev. A **59**, 169 (1999).
[27] J. Pan *et al.*, Nature (London) **410**, 1067 (2001).
[28] O. A. Collins *et al.*, Phys. Rev. Lett. **98**, 060502 (2007).